

Impact of Light Higgs Properties on the Determination of $\tan\beta$ and m_{susy}

Jun-ichi KAMOSHITA*

Department of Physics of Ochanomizu University, Tokyo 112-0012, Japan

Abstract

We examine whether parameters related to the Higgs sector of the minimal supersymmetric standard model can be determined by detailed study of the production cross section and decay branching ratios of the Higgs boson. Assuming that only the light Higgs boson will be observed at a future e^+e^- linear collider with $\sqrt{s} = 300 \sim 500$ GeV, we show that values of m_{susy} and $\tan\beta$ are restricted within a narrow region in the m_{susy} versus $\tan\beta$ plane by the combined analysis of the light Higgs properties. It is also pointed out that, in some case, $\tan\beta$ may be restricted to a relatively small value, $\tan\beta = 1 \sim 5$.

The minimal supersymmetric standard model (MSSM) is considered to be an attractive candidate as a theory beyond the standard model (SM). In the MSSM, the Higgs sector consists of two Higgs doublets, and there exist five physical states: two CP-even Higgs bosons (h and H with $m_h < m_H$), one CP-odd Higgs boson (A), and one pair of charged Higgs bosons (H^\pm). It is possible to derive specific predictions for this Higgs sector because the form of the Higgs potential in the MSSM is very restricted in comparison with that in the general two Higgs doublets model. In particular, the upper bound on the mass of the lightest CP-even neutral Higgs boson is predicted as about 130 GeV.[1] As for the detectability of the Higgs boson, it has been shown that at least one CP-even neutral Higgs boson should be detectable at a future e^+e^- linear collider with $\sqrt{s} = 300 \sim 500$ GeV.[2] Furthermore, the detectability of the Higgs boson is claimed for a large class of SUSY standard models with extended Higgs sectors.[3]

Once the Higgs boson is discovered, one of the questions of interest is to what extent the parameters related to the Higgs sector will be constrained from the detailed study of properties of the Higgs boson. By branching ratios of the Higgs boson, the mass of a CP-odd Higgs boson (m_A) can be constrained almost independently of the SUSY breaking mass scale (m_{susy}) even if the CP-odd Higgs boson is not discovered at future linear colliders with $\sqrt{s} = 300$ GeV.[4]

In this paper we consider the determination of parameters of the Higgs sector in the MSSM assuming that only the lightest CP-even Higgs boson will be observed at a future e^+e^- linear collider with $\sqrt{s} = 300 \sim 500$ GeV. It is shown that the allowed m_{susy} - $\tan\beta$ parameter space can be restricted within a narrow region by precise measurements of Higgs boson properties.

Let us begin by listing the parameters of the Higgs sector and the observables which can be used to determine these parameters. At the tree level, the masses of Higgs bosons and the mixing angle among Higgs bosons are determined by two parameters, the CP-odd Higgs boson mass and the ratio of the vacuum expectation values ($\tan\beta = \frac{\langle H_2 \rangle}{\langle H_1 \rangle}$), where H_1 is a Higgs doublet that couples to up-type quarks and H_2 is a Higgs doublet that couples to down-type quarks and leptons. However, once the radiative corrections to the Higgs potential are taken into account, they bring out new parameters in our analysis. In the calculation of the Higgs effective potential at the one loop level, the most important contribution comes from the top and stop loop, and therefore the relevant parameters are two stop masses ($m_{\tilde{t}_1}, m_{\tilde{t}_2}$), a Higgsino mass parameter

*E-mail : kamosita@theory.kek.jp

(μ), and a trilinear soft-breaking parameter (A_t). For the moment, we assume that no significant effect is induced from the left-right mixing of the stop sector.¹ Then, effectively there are three parameters related to the Higgs sector. As usual, for these three parameters, we take m_A , $\tan \beta$, and m_{susy} defined by $m_{susy} = \sqrt{m_{\tilde{t}_1} m_{\tilde{t}_2}}$. Then the CP-even Higgs mass matrix[5] is

$$M_{\text{higgs}}^2 = \begin{pmatrix} m_Z^2 \cos^2 \beta + m_A^2 \sin^2 \beta & -(m_Z^2 + m_A^2) \cos \beta \sin \beta \\ -(m_Z^2 + m_A^2) \cos \beta \sin \beta & m_Z^2 \sin^2 \beta + m_A^2 \cos^2 \beta + \frac{\delta_t}{\sin^2 \beta} \end{pmatrix}, \quad (1)$$

where

$$\delta_t = \frac{3m_t^4}{4\pi^2 v^2} \ln \left(\frac{m_{susy}^2}{m_t^2} \right) \quad (2)$$

represents the leading part of the radiative corrections due to the top-stop loop effect, with $v = \sqrt{\langle H_2 \rangle^2 + \langle H_1 \rangle^2} \simeq 174$ GeV. The masses of CP-even Higgs bosons and the Higgs mixing angle, α , are given by

$$m_h^2 = \frac{1}{2} \left[m_A^2 + m_Z^2 + \delta_t / \sin^2 \beta - \sqrt{\{(m_Z^2 - m_A^2) \cos 2\beta - \delta_t / \sin^2 \beta\}^2 + (m_Z^2 + m_A^2)^2 \sin^2 2\beta} \right], \quad (3)$$

$$m_H^2 = m_A^2 + m_Z^2 - m_h^2 + \delta_t / \sin^2 \beta, \quad (4)$$

$$\tan \alpha = \frac{(m_Z^2 + m_A^2) \cos \beta \sin \beta}{m_h^2 - (m_Z^2 \cos^2 \beta + m_A^2 \sin^2 \beta)}. \quad (5)$$

The lightest CP-even Higgs boson is mainly produced through the Higgs-strahlung process, $e^+e^- \rightarrow Zh$, at a e^+e^- linear collider with $\sqrt{s} = 300 \sim 500$ GeV. If we assume that the decay modes of the Higgs boson to SUSY particles are not dominant,² then the main decay mode of the Higgs boson is the $h \rightarrow b\bar{b}$ mode. In this case, the behavior of the Higgs boson may be similar to that of a Higgs boson in the SM. The lightest Higgs boson then has sizable decay branching ratios in the modes $h \rightarrow b\bar{b}, \tau\bar{\tau}, c\bar{c}$ and gg .³

With a reasonable luminosity of $\sim 50 \text{ fb}^{-1}/\text{year}$, the mass of the Higgs boson, m_h , can be determined precisely by the recoil mass distribution.[6, 7, 8] The Higgs production cross section, $\sigma(e^+e^- \rightarrow Zh)$, is obtained by the branching ratio of the Z boson decaying into $l\bar{l}$ ($l = e, \mu$) and the cross section of the event with the recoil mass around m_h . [7] The production cross section multiplied by the branching ratio of $h \rightarrow X$ ($X = \{b\bar{b}\}, \{\tau\bar{\tau}\}, \{c\bar{c} \text{ or } gg\}$),⁴ $\sigma(e^+e^- \rightarrow Zh) Br(h \rightarrow X)$, can be obtained by the ZX production rate with the invariant mass of X being around m_h . [7, 8]

The three parameters m_A , $\tan \beta$ and m_{susy} will be restricted by the observables mentioned above. Expected experimental errors of observables have been estimated in detail.[8] According to these estimates, the error of m_h should be $0.1 \sim 0.5\%$. Therefore, in the following, we treat the value of m_h as fixed. Thus there are two remaining degrees of freedom of parameters. Hereafter we choose m_{susy} and $\tan \beta$ as free parameters and derive the value of m_A with the Higgs mass formula Eq. (3) for the fixed value of m_h . For $m_h = 120$ GeV, Fig. 1 displays the contour plot of m_A in the m_{susy} - $\tan \beta$ plane.

¹ In our analysis, we use the Higgs mass matrix including the L - R mixing effect of two stops.[5]

² If decays of the Higgs boson to the SUSY particles are observed, we can see obviously that the Higgs boson belongs to the SUSY model. We will not consider such a case because we are now interested in the case that the SM-like Higgs boson will be observed.

³ Since the availability of $h \rightarrow WW^*$ depends crucially on the Higgs boson mass, we will not consider this mode here.

⁴ Although it is very difficult to measure the branching ratios of the modes $c\bar{c}$ and gg separately, the sum of $Br(h \rightarrow c\bar{c})$ and $Br(h \rightarrow gg)$ can be measured with reasonable precision.[7, 8, 9, 10] We denote the sum of $Br(h \rightarrow c\bar{c})$ and $Br(h \rightarrow gg)$ as $Br(h \rightarrow c\bar{c} \text{ or } gg)$.

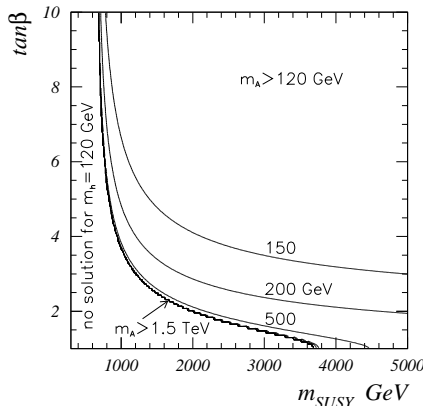


Figure 1: Contour plots of the value of m_A for $m_h = 120$ GeV are shown in the m_{susy} versus $\tan\beta$ plane. We take the top quark mass as $m_t = 175$ GeV. The Higgs mass formula Eq.(3) can not be satisfied for $m_h = 120$ GeV in the left and bottom left region in the figure. In large $\tan\beta$ and large m_{susy} region, the value of m_A is always larger than 120 GeV when $m_h = 120$ GeV.

Table 1: Couplings of the light Higgs boson to a fermion pair in the MSSM and the SM. u, d and l represents up-type quarks ($u = \{u, c, t\}$), down-type quarks ($d = \{d, s, b\}$), and leptons ($l = \{e, \mu, \tau\}$).

	$h-u-u$	$h-d-d$	$h-l-l$
MSSM	$-i \frac{m_u}{v} \frac{\cos \alpha}{\sin \beta}$	$i \frac{m_d}{v} \frac{\sin \alpha}{\cos \beta}$	$i \frac{m_l}{v} \frac{\sin \alpha}{\cos \beta}$
SM	$-i \frac{m_u}{v}$	$-i \frac{m_d}{v}$	$-i \frac{m_l}{v}$

The ratio of branching ratios, for example $Br(h \rightarrow c\bar{c} \text{ or } gg)/Br(h \rightarrow b\bar{b})$, will be determined with reasonable precision.[7, 8, 10] The formulas for the partial decay width of the Higgs boson in the MSSM are derived, for example, in Ref. [11]. Higgs-fermion-fermion couplings are listed in Table 1. The partial decay width for $h \rightarrow b\bar{b}$ and $h \rightarrow \tau\bar{\tau}$ are proportional to the down-type fermion-Higgs coupling, and then the ratio $Br(h \rightarrow \tau\bar{\tau})/Br(h \rightarrow b\bar{b})$ is the same as that in the SM. Therefore no information on the parameters of the Higgs sector in the MSSM are obtained from this ratio.⁵ On the other hand, as reported in Ref. [4], the ratio $Br(h \rightarrow c\bar{c} \text{ or } gg)/Br(h \rightarrow b\bar{b})$ is a useful variable to constrain the value of m_A , because the ratio strongly depends on m_A but is almost independent of m_{susy} .

The determination of $\tan\beta$ has great implication for both the theoretical and experimental study of SUSY standard models, because not only the physics of the Higgs sector but also that of other SUSY sectors, for example the chargino and neutralino sector, depend on $\tan\beta$. Therefore we must start to use other observables in order to determine the values of both m_{susy} and $\tan\beta$.

Hereafter we use abbreviated notation defined as follows: $\sigma_{Zh} \equiv \sigma(e^+e^- \rightarrow Zh)$, $\sigma_{Zh}Br(b\bar{b}) \equiv \sigma(e^+e^- \rightarrow Zh)Br(h \rightarrow b\bar{b})$ and $R_{br} \equiv Br(h \rightarrow c\bar{c} \text{ or } gg)/Br(h \rightarrow b\bar{b})$. These observables give us different constraints on the values of m_{susy} and $\tan\beta$. As discussed in Ref. [4], we obtain the

⁵ This ratio is important to determine the bottom mass, as discussed, for example, in Refs. [4, 8].

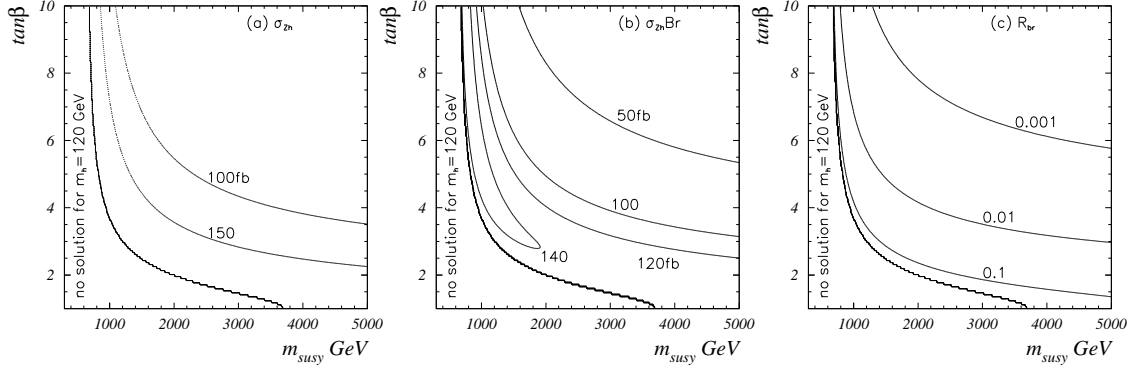


Figure 2: Contours plots of (a) σ_{Zh} , (b) $\sigma_{Zh}Br(b\bar{b})$, and (c) R_{br} are shown. We take the quark masses as $m_t = 175$ GeV, $m_b(m_b) = 4.2$ GeV and $m_c(m_c) = 1.3$ GeV. The strong coupling constant is taken as $\alpha_s(m_Z) = 0.12$.

approximate relation

$$R_{br} \propto \left(\frac{1}{\tan \beta \tan \alpha} \right)^2.$$

Both $\sigma(e^+e^- \rightarrow Zh)$ and $\sigma(e^+e^- \rightarrow Zh)Br(h \rightarrow b\bar{b})$ depend on the angles α and β as

$$\begin{aligned} \sigma_{Zh} &\propto \sin^2(\alpha - \beta), \\ \sigma_{Zh}Br(b\bar{b}) &\propto \sin^2(\alpha - \beta) \left(1 + \frac{m_\tau^2}{3m_b^2} + R_{br} + f(\alpha, \beta) \right)^{-1}, \end{aligned}$$

where

$$f(\alpha, \beta) \equiv \left(\Gamma_{\text{tot}} - \sum_X \Gamma(h \rightarrow X) \right) / \Gamma(h \rightarrow b\bar{b}), \quad (6)$$

$X = b\bar{b}, \tau\bar{\tau}, c\bar{c}, gg$. Here Γ_{tot} is the total decay width of the light Higgs boson. In Fig. 2(a)~(c) display the contour plots of σ_{Zh} , $\sigma_{Zh}Br(b\bar{b})$ and R_{br} , respectively, in the $m_{\text{susy}}\text{-tan } \beta$ plane for $m_h = 120\text{GeV}$. The shape of the contours in Fig. 2(b) is somewhat different from the other two in the left side of the figure. Fig. 2(a) for σ_{Zh} is similar to Fig. 2(c) for R_{br} . However, Fig. 2(a) displays gentle slope, as compared with Fig. 2(c).

Now we combine these observables to estimate the constraints on the values of m_{susy} and $\tan \beta$. For this purpose, we take m_{susy} and $\tan \beta$ as fitting parameters and then perform the χ^2 test in the $m_{\text{susy}}\text{-tan } \beta$ plane for a fixed value of m_h . The value of m_A is derived from the Higgs mass formula Eq.(3) point-by-point in the $m_{\text{susy}}\text{-tan } \beta$ plane.

However, we input the values of m_h , m_A^0 and m_{susy}^0 as true values for the χ^2 test,⁶ because these variables have clear physical meanings as the mass of particles and a typical mass scale for m_{susy} . As for $\tan \beta$, the ‘‘true’’ value is calculated from the input parameters, m_h , m_A^0 and m_{susy}^0 , by the Higgs mass formula Eq. (3).

Definition of χ^2 is given by

$$\chi^2 \equiv \left\{ \left(\frac{\sigma_{Zh} - \sigma_{Zh}^0}{\delta\sigma_{Zh}} \right)^2 + \left(\frac{\sigma_{Zh}Br(b\bar{b}) - \sigma_{Zh}Br(b\bar{b})^0}{\delta(\sigma_{Zh}Br(b\bar{b}))} \right)^2 + \left(\frac{R_{br} - R_{br}^0}{\delta(R_{br})} \right)^2 \right\}, \quad (7)$$

⁶ In order to distinguish ‘‘true’’ values of m_A and m_{susy} from m_A and m_{susy} as fitting parameters, the index ‘‘0’’ is appended to the ‘‘true’’ values.

Table 2: List of errors for each observable discussed in Ref. [8]. R_{br} is defined by $R_{br} \equiv Br(h \rightarrow c\bar{c} \text{ or } gg)/Br(h \rightarrow b\bar{b})$ [4].

m_h	$\delta(m_h)$	$\delta(\sigma_{Zh})$	$\delta(\sigma_{Zh}Br(bb))$	$\delta(R_{br})$
110 GeV	0.1 \sim 0.5%	\sim 7%	\sim 2.5%	\sim 14%
120 GeV	0.1 \sim 0.5%	\sim 7%	\sim 3.5%	\sim 14%

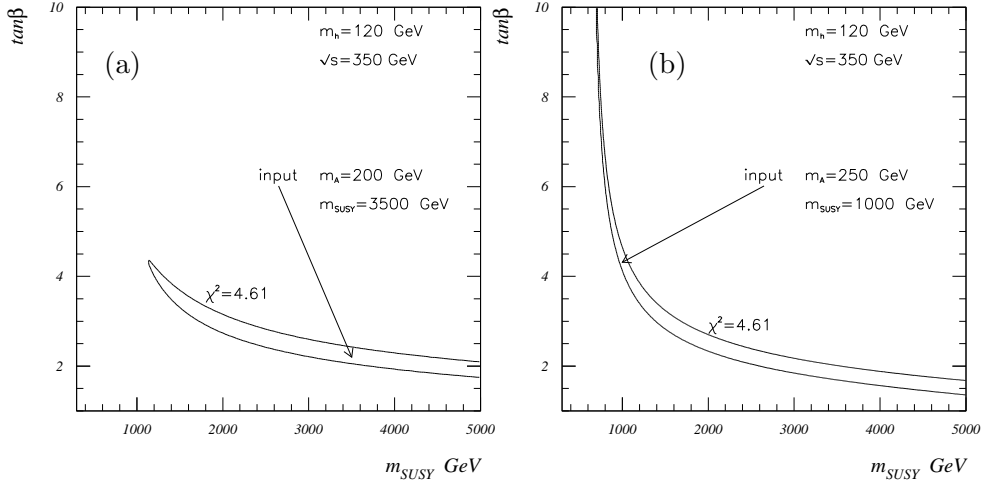


Figure 3: Contour plot of χ^2 with $\chi^2 = 4.61$ (a) for $(m_h, m_A^0, m_{susy}^0) = (120 \text{ GeV}, 200 \text{ GeV}, 3500 \text{ GeV})$ and (b) for $(m_h, m_A^0, m_{susy}^0) = (120 \text{ GeV}, 250 \text{ GeV}, 1000 \text{ GeV})$. $\chi^2 < 4.61$ inside a narrow region.

where $\delta(\sigma_{Zh})$, $\delta(\sigma_{Zh}Br(bb))$ and $\delta(R_{br})$ represent expected experimental errors. The estimated error of each observable reported in Ref. [8] is summarized in Table 2. σ_{Zh}^0 , $\sigma_{Zh}Br(bb)^0$ and R_{br}^0 are the central values derived from the input parameters, m_h , m_A^0 and m_{susy}^0 . The values of σ_{Zh} , $\sigma_{Zh}Br(bb)$ and R_{br} are calculated at each point in the m_{susy} versus $\tan \beta$ plane. To calculate the Higgs production cross section, we use $\sqrt{s} = 350 \text{ GeV}$.⁷

The contour plots of χ^2 for $m_h = 120 \text{ GeV}$ are shown in Figs. 3(a) and (b) with a 95%CL contour. We find in Fig. 3(a) that the $\tan \beta$ is restricted within a relatively small value, $\tan \beta < 4.5$, and the value of m_{susy} is weakly restricted, $m_{susy} > 1 \text{ TeV}$. Fig. 3(b) displays the contour plot of χ^2 for other input value. In Fig. 3(b), although the upper bounds on m_{susy} and $\tan \beta$ are not obtained in the displayed region, the allowed m_{susy} - $\tan \beta$ parameter space is restricted within a narrow region.

Next, in order to show how each observable contributes to constrain the m_{susy} - $\tan \beta$ parameter space, we show the χ^2 contour plots in Fig. 4 by using just two observables among the three observables. We can see from Fig. 4 that R_{br} contributes strongly to the constraint on the m_{susy} - $\tan \beta$ plane.

The results above can be understood as follows. Once the value of m_h is fixed, $\tan \beta$ and m_{susy} are strongly correlated by the Higgs mass formula Eq. (3). We can consider Fig. 1 as showing the value of $\tan \beta$ as a function of m_{susy} for fixed values of m_h and m_A . From Fig. 1, the m_{susy} - $\tan \beta$ parameter space is restricted within a relatively narrow region even if m_A varies

⁷ Of course when $m_A < \sqrt{s}/2$, the CP-odd Higgs boson will be produced by an associated production process, $e^+e^- \rightarrow AH$. In this case we can use many observables depending on SUSY parameters and should convert the strategy of our analysis to another one. Since we assume that only a light Higgs boson will be discovered, we constrain our analysis to $m_A > \sqrt{s}/2 \sim 180 \text{ GeV}$. Hereafter we will not consider the case $m_A < 180 \text{ GeV}$.

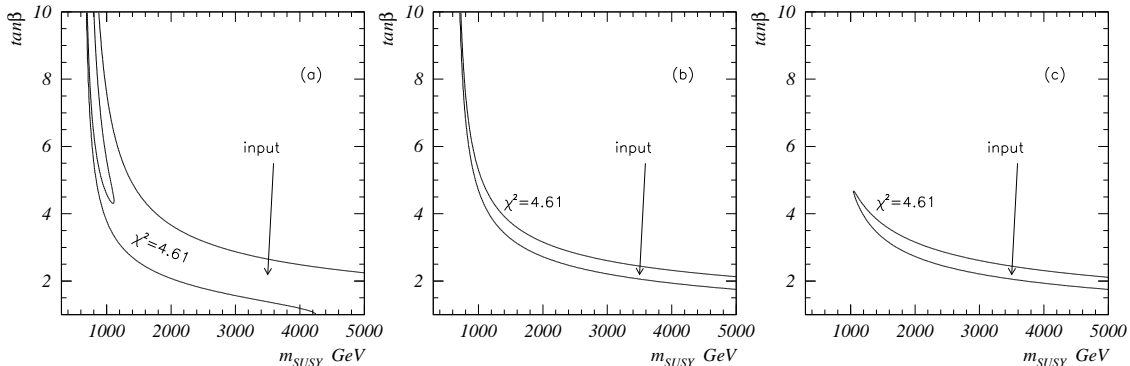


Figure 4: Contour plots of χ^2 with $\chi^2 = 4.61$ when we use just two observables among σ_{Zh} , $\sigma_{Zh}Br(b\bar{b})$ and R_{br} : (a) σ_{Zh} and $\sigma_{Zh}Br(b\bar{b})$, (b) σ_{Zh} and R_{br} , (c) $\sigma_{Zh}Br(b\bar{b})$ and R_{br} . Input values of the parameters are taken to be the same as in Fig. 3(a).

from ~ 200 GeV to larger than 1 TeV. However the constraint obtained from Fig. 1 is weak as compared with that from Fig. 3(a) and (b). We can see from Fig. 4 that R_{br} contributes strongly to the constraint on the m_{susy} - $\tan\beta$ plane. In Figs. 3(a) and 4, the value of m_A is restricted within about 180~230 GeV by R_{br} , and as a result the region satisfying the constraints becomes narrow as compared with that obtained in Fig. 1. The reason why the upper bound on $\tan\beta$ is obtained in Fig. 3(a) is, in addition to R_{br} , $\sigma_{Zh}Br(b\bar{b})$ contributes effectively to the constraint on the m_{susy} - $\tan\beta$ plane.

So far, we have neglected the L - R mixing of the stop sector. We can include the L - R mixing effects and take non-zero values of A_t and μ in our analysis. In this case, examples are shown in Fig. 5. The contour should be shifted by varying the values of A_t and μ . However, the result of our analysis will not change essentially, because R_{br} is almost independent of the parameters of the stop sector, as shown in Ref. [4].

With regard to theoretical aspects, the requirement of Yukawa coupling unification in SUSY-GUT[12] restricts the value of $\tan\beta$ to two solutions. One is the small $\tan\beta$ solution, $\tan\beta = 1 \sim 3$, and the other one is the large $\tan\beta$ solution, $\tan\beta \sim 50$. There are mainly two types of scenarios for Yukawa coupling unification. These are the bottom-tau Yukawa unification and the top-bottom-tau Yukawa unification scenarios. The requirement of bottom-tau Yukawa coupling unification suggests both the small $\tan\beta$ solution and the large $\tan\beta$ solution. However, the requirement of top-bottom-tau Yukawa coupling unification suggests only the large $\tan\beta$ solution. Therefore, if a large value of $\tan\beta$ will be excluded by precise measurements of light Higgs properties at a future linear collider, for example as we have shown in Fig. 3(a), the experiments may rule out the top-bottom-tau Yukawa unification scenario even if only the lightest CP-even Higgs boson is observed.

We now conclude our discussion. We have examined whether the parameters of the Higgs sector in the MSSM can be determined by detailed study of Higgs properties. We have found that the values of $\tan\beta$ and m_{susy} are restricted within a very narrow region even if only the light Higgs boson is discovered. R_{br} contributes strongly to the constraint on the m_{susy} - $\tan\beta$ plane. We also have shown that the upper bound on $\tan\beta$ may be obtained by combining analysis of observables when $\sigma_{Zh}Br(b\bar{b})$ contributes effectively to the constraint. However, to obtain a more strict constraint on both m_{susy} and $\tan\beta$, we need constraints inferred from other quantities obtained from heavy Higgs and/or SUSY particles.

The author would like to thank A. Sugamoto, S. Kamei and M. Aoki for reading the manuscript and helpful comments.

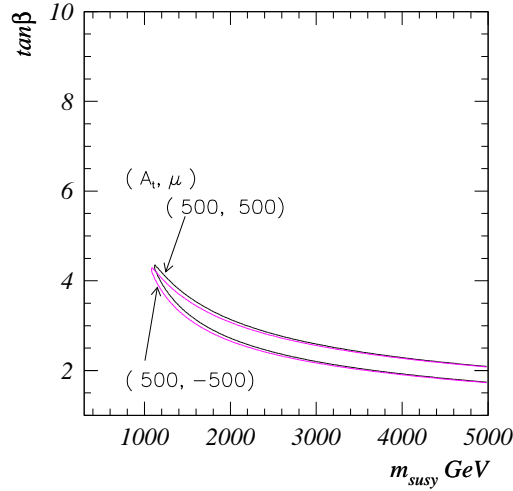


Figure 5: Contour plots of χ^2 with $\chi^2 = 4.61$ including the L-R mixing effect of two stops. The values shown in the parenthesis represent (A_t, μ) in GeV. Input values of other parameters are taken to be the same as in Fig. 3(a).

References

- [1] Y. Okada, M. Yamaguchi and T. Yanagida, *Prog. Theor. Phys.* **85** (1991), 1; *Phys. Lett.* **B262** (1991), 54.
J. Ellis, G. Ridolfi and F. Zwirner, *Phys. Lett.* **B257** (1991), 83.
H. E. Haber and R. Hempfling, *Phys. Rev. Lett.* **66** (1991), 1815.
- [2] P. Janot, Workshop, Saariselka, Finland, Sep 9-14, 1991. In *Munich/Annecy/Hamburg 1991, Proceedings, "e⁺e⁻ collisions at 500 GeV"*, pp. 107-131.
J. Kamoshita, INS Workshop, Dec 20-22, 1994, *Proceedings, "Physics of e⁺e⁻, e⁻ γ and $\gamma\gamma$ collisions at linear accelerators"*, INS-J-181.
- [3] J. Kamoshita, Y. Okada, M. Tanaka, *Phys. Lett.* **B328** (1994), 67.
- [4] J. Kamoshita, Y. Okada, M. Tanaka, *Phys. Lett.* **B391** (1997), 124.
- [5] J. Ellis, G. Ridolfi and Zwirner, *Phys. Lett.* **B257** (1991), 83.
- [6] JLC-I, KEK Report 92-16, December 1992.
- [7] See, for example, J. F. Gunion, A. Stange and S. Willenbrock, hep/ph9602238, UCD-95-28.
- [8] J. F. Gunion et al. hep/ph9703330, "Proceedings of the 1996 DPF/DPB Summer Study on New Directions for High Energy Physics (Snowmass 96)", UCD-97-5.
- [9] M. D. Hildrech, T. L. Barklow and D. L. Burke *Phys. Rev.* **D49** (1994), 3441.
- [10] K. Kawagoe, I. Nakamura, *Phys. Rev.* **D54** (1996), 3634 .
- [11] V. Barger, M. S. Berger, A. L. Stange and R. J. N. Phillips, *Phys. Rev.* **D45** (1992), 4128.
A. Djouadi, J. Kalinowski, P. M. Zerwas, *Z. Phys.* **C70** (1996), 435.
- [12] B. Pendleton and G. G. Ross *Phys. Lett.* **B98** (1981), 291.
V. Barger, M. S. Berger, P. Ohmann, and R. N. Phillips *Phys. Lett.* **B314** (1993), 351.
P. Langacker, N. Polonsky, *Phys. Rev.* **D49** (1994), 1454.
S. Kelley, J. L. Lopez and D. V. Nanopoulos *Phys. Lett.* **B274** (1992), 387.
M. Carena, M. Olechowski, S. Pokorski and C. E. M. Wagner *Nucl. Phys.* **B426** (1994), 269.